Medicinal Chemistry Research
https://doi.org/10.1007/s00044-018-2242-5

MEDICINAL CHEMISTRY RESEARCH

ORIGINAL RESEARCH

Cytotoxicity, apoptosis, and QSAR studies of phenothiazine derived methoxylated chalcones as anticancer drug candidates

Halise Inci Gul[1] · Cem Yamali[1] · Gulsen Gunesacar[1,2] · Hiroshi Sakagami[3,4] · Noriyuki Okudaira[4] · Yoshihiro Uesawa[5] · Hajime Kagaya[5]

Received: 21 May 2018 / Accepted: 25 August 2018

Abstract

In the present study, chalcones "(*E*)-1-(10*H*-phenothiazine-2-yl)-3-aryl-prop-2-en-1-ones, **FS1-11**" were successfully synthesized via base-catalyzed Claisen–Schmidt condensation. Chemical structures of the compounds were confirmed by ^{1}H NMR, ^{13}C NMR, and HRMS techniques. Aryl part of the chalcone was changed as mono, di, and trimethoxylated phenyls. Cytotoxicities of the phenothiazine derivatives were evaluated against four human oral squamous cell carcinoma (OSCC) cell lines (Ca9-22, HSC-2, HSC-3, and HSC-4) and three human normal oral cells (HGF, HPLF, and HPC) by MTT test. The CC_{50} values of the compounds were calculated in the range of 0.9–109.8 μM towards OSCC malign cell lines. Trimethoxylated compound **FS6**, (*E*)-1-(10*H*-phenothiazine-2-yl)-3-(2,4,5-trimethoxyphenyl)-prop-2-en-1-one, was found the most selective cytotoxic compound among the series with the highest selectivity index (SI) (SI = 76.5) and potency-selectivity expression (PSE) (PSE = >1285; > 1602) values. Western blot analysis demonstrated that **FS6** (8–64 μM) induced the production of cleaved product of PARP and the activation of caspase-3 in HSC-2 cells, suggesting the induction of apoptosis by **FS6**. QSAR analysis suggested that the tumor specificity of the chalcones correlated with their molecular shape, volume, and electrostatic properties.

Keywords Phenothiazine · Chalcone · Anticancer · Apoptosis · PARP · QSAR

Introduction

Cancer is one of the major causes of death worldwide (Thun et al. 2010). According to World Health Organisation (WHO) cancer report 2014, cancer incidence is expected to increase 57% worldwide in the next 20 years. By 2030, it is estimated that there will be almost 26 million new cancer cases and 17 million cancer deaths per year (Thun et al. 2010). There are many types of anticancer drugs in the clinic (Raghavendra et al. 2018). However, chemotherapeutic drugs have several adverse effects such as nausea, vomiting, hair loss, and pain, and so many cancer patients undergo great suffering during treatment (Raghavendra et al. 2018). Their associated limitations and adverse effects are still prompting the researchers to develop more safe, potent, and selective anticancer drug candidates.

Among the currently identified drug candidates, chalcones are an important class of phytochemicals that have received much attention due to their wide range of biological activities such as anticancer, antimalarial, antimicrobial, antiinflammatory, anti-HIV, and antioxidant effects (Yerdelen et al. 2015; Yamali et al. 2016; Yamali et al. 2017a; Tugrak et al. 2016; Singh et al. 2014; Gul et al. 2007; Gul et al. 2008; Gul et al. 2009; Gomes et al. 2017; Das et al. 2006; Yamali et al. 2017b).

Chalcones are open-chain molecules bearing two aromatic rings linked by a three-carbon enone fragment (Singh et al. 2014). The presence of double bond in conjugation with carbonyl functionality is believed to be responsible for the biological activities of chalcones since removal of this functionality make them inactive (Singh et al. 2014).

✉ Halise Inci Gul
incigul1967@yahoo.com

[1] Faculty of Pharmacy, Department of Pharmaceutical Chemistry, Ataturk University, Erzurum, Turkey

[2] Faculty of Pharmacy, Department of Pharmaceutical Chemistry, Erzincan University, Erzincan, Turkey

[3] Division of Pharmacology, Meikai University School of Dentistry, Saitama, Sakado, Japan

[4] Meikai University Research Institute of Odontology (M-RIO), Meikai University School of Dentistry, Saitama, Sakado, Japan

[5] Department of Clinical Pharmaceutics, Meiji Pharmaceutical University, Kiyose, Tokyo, Japan

Published online: 08 September 2018

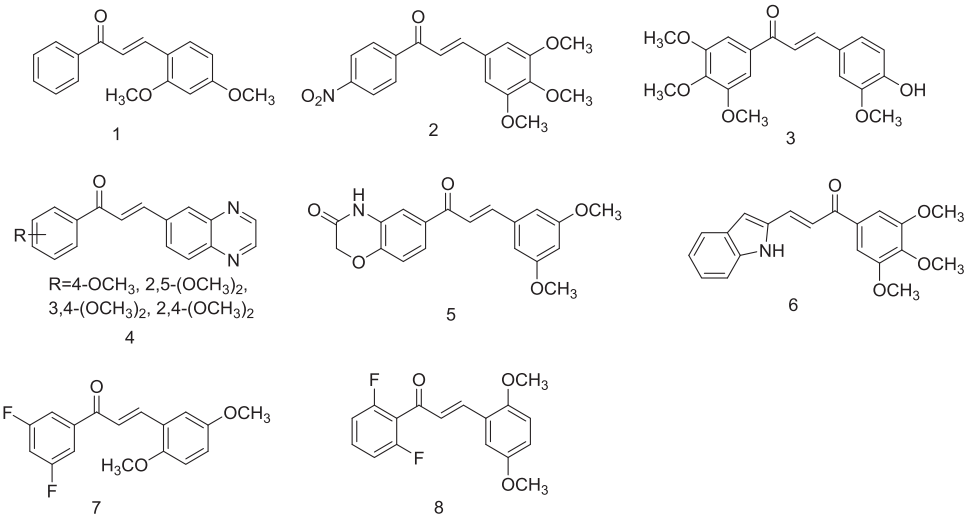

Fig. 1 Several chalcones with anticancer properties **1**–**6** (Singh et al. 2014), **7** (Yamali et al. 2017a), **8** (Yamali et al. 2017b)

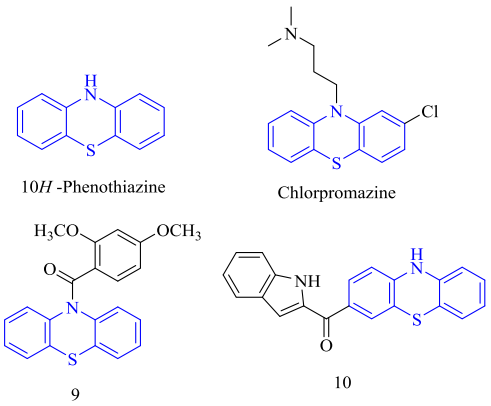

Fig. 2 Phenothiazine derivatives as anticancer compounds

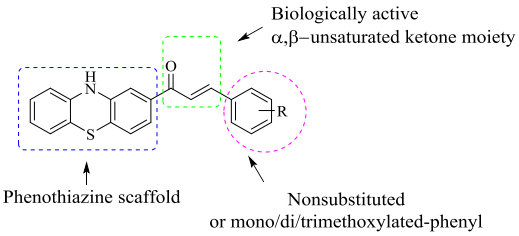

Fig. 3 General chemical structure of targeted chalcones **FS1**–**11** bearing phenothiazine scaffold. R=H or -OCH_3 group/s on suitable position/s

Recently, studies have focused on the antiproliferative and anticancer properties of the chalcones (Yerdelen et al. 2015; Yamali et al. 2016; Yamali et al. 2017a; Tugrak et al. 2016; Singh et al. 2014; Mahapatra et al. 2015; Gul et al. 2007, 2008, 2009; Gomes et al. 2017; Das et al. 2006; Yamali et al. 2017b; Badr et al. 2018). Several compounds (Fig. 1) possessing polymethoxy groups and/or heterocyclic ring were reported with cytotoxic/anticancer activities.

Phenothiazine, a sulfur and nitrogen-containing tricyclic scaffold, was reported with a wide range of pharmacological activity spectrum including anticancer, antibacterial, antipsychotic, and multi-drug resistance (MDR) reversal effects (Fig. 2) (Ohlow and Moosmann 2011; Pluta et al. 2011). Phenothiazine drugs are relatively stable and widely used as antipsychotic drugs (Varga et al. 2017). Studies on chlorpromazine (Fig. 2), a representative drug having phenothiazine pharmacophore, showed that chlorpromazine can enhance the cytotoxic effects of tamoxifen on breast cancer (Yde et al. 2009). Phenothiazines can also enhance the sensitivity of chemotherapy drugs such as cisplatin (Eriksson et al. 2001). In particular new phenothiazine derivatives, **9** and **10** (Fig. 2), have been evaluated for their ability to inhibit tubulin polymerization and antiproliferative activity against 60 cancer cell lines (Ghinet et al. 2016). The compounds at issue showed impressive cell growth inhibition on human colon Duke's type D, colorectal adenocarcinoma COLO 205, and human kidney adenocarcinoma A498 cell lines (Ghinet et al. 2016). These remarkable findings suggested that phenothiazine moiety can be considered as a promising anticancer pharmacophore in medicinal chemistry. In recent years, the concept of hybrid drugs has gained more attention in which two or more pharmacophores are linked covalently to a single molecule (Meunier 2008). It is expected that this approach may solve the problem of drug resistance by showing dual drug action (Meunier 2008).

Our research group has previously shown that a set of chalcones containing polymethoxy phenyl moiety had a selective anticancer activity against human oral squamous cell carcinoma (OSCC) cell lines (Yamali et al. 2017a, 2017b). These findings prompted us to synthesize new methoxylated chalcones bearing phenothiazine ring as hybrid molecules "(*E*)-1-(10*H*-phenothiazine-2-yl)-3-aryl-prop-2-en-1-ones, **FS1**-**11**" (Fig. 3) and to evaluate designed compounds as anticancer agents towards human OSCC and human normal oral cells by MTT method. In

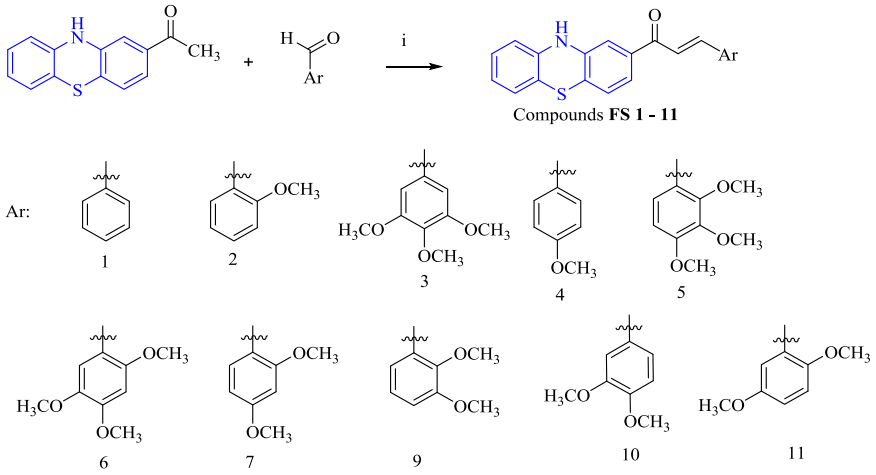

Scheme 1 Synthesis of the compounds **FS1–11**. i: Methanol, aqueous solution of KOH (40%), reflux, 3 h, 70 °C

addition, it was also aimed to investigate the possible mechanism of action of the compounds in cytotoxicity and analyse the results using quantitative structure-activity relationship (QSAR) analysis.

Material and methods

Chemistry

Nuclear magnetic resonance (NMR) spectra (^{1}H NMR and ^{13}C-NMR) of the compounds were recorded with DPX 300 NMR spectrometer (Bruker Bioscience, Billerica, MA, USA) and Bruker AVANCE III 400 MHz (Bruker, Karlsruhe, Germany) spectrometer in dimethyl sulfoxide (DMSO)-d_6. Chemical shifts (δ) were reported in ppm. High-Resolution Mass Spectra (HRMS) of the compounds were taken using a liquid chromatography ion trap-time of the flight tandem mass spectrometer (Shimadzu, Kyoto, Japan) equipped with an electrospray ionization (ESI) source, operating in both positive and negative ionization mode. Shimadzu's LCMS Solution software was used for data analysis. Melting points were determined using an Electrothermal 9100 instrument (IA9100, Bibby Scientific Limited, Staffordshire, UK) and are uncorrected. Process of the reaction was monitored by Thin Layer Chromatography (TLC) using Silicagel HF_{254} (Merck Art 5715) plate under UV lamb (254 and 365 nm, Spectroline, Model ENF-240C/FE, Spectronics Corporation Westbury, New York U.S.A).

General synthesis of (*E*)-1-(10*H*-phenothiazine-2-yl)-3-aryl-prop-2-en-1-ones, compounds FS1-11, Scheme 1

Targeted chalcones in this study **FS1–11** were synthesized according to literature with some minor modifications (Bansode and Meshram 2012; Do et al. 2016; Ranganathan et al. 2013; Saranya and Ravi 2014). To the mixture of 2-acetylphenothiazine (4.14 mmol) and a suitable benzaldehyde (4.14 mmol) in methanol (20 ml), an aqueous solution of KOH (40%, 4 ml) was added and the mixture was refluxed for 3 h at 70 °C. Reactions were followed by TLC ($CHCl_3$). The reaction mixture was then cooled to room temperature and poured on to crushed ice containing few drops of concentrated HCl (37%) solution and left overnight in a cooler. The solid precipitated was filtered and washed with cold methanol. The compounds were purified by crystallization. Solvent system used in crystallization was EtOH/DMF/water (**FS1**, **FS4**, and **FS6**), MeOH/$CHCl_3$ (**FS2** and **FS7**), MeOH/DMF (**FS5**), DMF/water (**FS9** and **FS10**), methanol (**FS3**), and acetonitrile/DMF (**FS11**).

(*E*)-1-(10*H*-Phenothiazine-2-yl)-3-phenyl-prop-2-en-1-one (FS1)

Claret red solid. Yield: 57.6% (64%, Saranya and Ravi 2013). Melting point (m.p.): 227–228.3 °C. ^{1}H NMR (DMSO-d_6, δ ppm, 300 MHz): 8.79 (s, 1H, NH), 7.87–7.82 (m, 2H, ArH), 7.75 (d, $J = 10.5$ Hz, 2H, ArH), 7.62 (dd, $J = 8.1$, 1.8, 1H, ArH), 7.47–7.45 (m, 3H, ArH), 7.31 (d, $J = 1.7$ Hz, 1H), 7.08 (d, $J = 8.0$ Hz,1H, ArH), 7.00 (td, $J = 7.8$, 1.5 Hz, 1H, ArH), 6.77 (dd, $J = 7.7$, 1.3 Hz, 1H, ArH), 6.76 (td, $J = 7.5$, 1.2 Hz, 1H, ArH), 6.66 (dd, $J = 7.9$,1.1 Hz, 1H, ArH). ^{13}C NMR (DMSO-d_6, δ ppm, 75 MHz): 188.5 (C=O), 144.2, 142.6, 141.6, 137.3, 135.1, 131.1,129.4, 129.3, 128.5, 126.7, 126.6, 124.1, 123.0, 122.6, 122.3, 115.7, 115.1, 113.4. HRMS (ESI-MS) Calc. for $C_{21}H_{16}NOS$ $[M+H]^+$, 329.0869; found 329.0863.

(*E*)-1-(10*H*-Phenothiazine-2-yl)-3-(2-methoxyphenyl)-prop-2-en-1-one (FS2)

(Ranganathan et al. 2013) Claret red solid. Yield: 20.8 %. Melting point (m.p.): 221.1–222 °C. ^{1}H NMR (DMSO-d_6, δ

ppm, 300 MHz): 8.79 (s, 1H, NH), 8.00 (d, $J = 15.8$, 1H, $H_ß$), 7.92 (dd, $J = 7.7$, 1.5 Hz, 1H, ArH), 7.74 (d, $J = 15.8$ Hz, 1H, $H_α$), 7.56 (dd, $J = 8.1$, 1.7 Hz, 1H, ArH), 7.48–7.42 (m, 1H, ArH), 7.30 (d, $J = 1.7$ Hz, 1H, ArH), 7.11 (d, $J = 8.2$ Hz, 1H, ArH), 7.10 (d, $J = 8.1$ Hz, 1H, ArH), 7.01 (d, $J = 7.5$ Hz, 2H, ArH), 6.91 (dd, $J = 7.7$, 1.2 Hz, 1H, ArH), 6.76 (td, $J = 7.5$, 1.1 Hz, 1H, ArH), 6.66 (dd, $J = 7.9$, 0.9 Hz, 1H, ArH), 3.90 (s, 3H, OCH_3). ^{13}C NMR (DMSO-d_6, δ ppm, 75 MHz): 188.5 (C=O), 158.8, 142.6, 141.6, 138.8, 137.5, 132.8, 129.0, 128.5, 126.7, 126.6, 123.9,123.4, 122.9, 122.6, 122.1, 121.2, 115.7, 115.1, 113.4, 112.3, 56.2. HRMS (ESI-MS) Calc. for $C_{22}H_{18}NO_2S$ $[M+H]^+$, 359.0975; found 359.0977.

(*E*)-1-(10*H*-Phenothiazine-2-yl)-3-(3,4,5-trimethoxyphenyl)-prop-2-en-1-one (FS3)

Violet solid. Yield: 21.4 %. Melting point (m.p.): 226.3–226.7 °C. ^{1}H NMR (DMSO-d_6, δ ppm, 400 MHz): 8.78 (s, 1H, NH), 7.75–7.60 (m, 3H, ArH), 7.27 (s, 1H, ArH), 7.18 (s, 2H, ArH), 7.06 (d, $J = 8.1$ Hz, 1H, ArH), 7.00–6.96 (m, 1H, ArH), 6.89 (d, $J = 7.7$ Hz, 1H, ArH), 6.74 (t, $J = 7.5$ Hz, 1H, ArH), 6.64 (d, $J = 8.1$ Hz, 1H, ArH), 3.69 (s, 3H, OCH_3), 3.32 (s, 6H, OCH_3). ^{13}C NMR (DMSO-d_6, δ ppm, 100 MHz): 188.7 (C=O), 153.8, 145.0, 142.8, 141.8, 137.7, 130.9, 128.7, 127.0, 126.7, 124.2, 123.3, 122.8, 121.7, 115.9, 115.3, 113.6, 107.2, 60.8, 56.8. HRMS (ESI-MS) Calc. for $C_{24}H_{22}NO_4S$ $[M+H]^+$, 420.1264; found 420.1251.

(*E*)-1-(10*H*-Phenothiazine-2-yl)-3-(4-methoxyphenyl)-prop-2-en-1-one (FS4)

Red solid. Yield: 21.4 % (66 %, Saranya and Ravi 2013). Melting point (m.p.): 226.3–226.7 °C. ^{1}H NMR (DMSO-d_6, δ ppm, 300 MHz): 8.78 (s, 1H, NH), 7.82 (d, $J = 8.9$ Hz, 2H, ArH), 7.66 (d, $J = 4.9$ Hz, 2H, ArH), 7.60 (dd, $J = 8.1$, 1.7 Hz, 1H, ArH), 7.30 (d, $J = 1.8$ Hz, 1H, ArH), 7.04 (d, $J = 15.5$ Hz, 1H), 6.99 (dd, $J = 7.2$, 1.2 Hz, 3H, ArH), 6.91 (dd, $J = 7.7$, 1.4 Hz, 1H, ArH), 6.75 (td, $J = 7.5$, 1.2 Hz, 1H, ArH), 6.66 (dd, $J = 7.9$, 1.4 Hz, 1H, ArH), 3.82 (s, 3H, OCH_3). ^{13}C NMR (DMSO-d_6, δ ppm, 75 MHz): 188.3 (C=O), 161.9, 144.2, 142.6, 141.7, 137.6, 131.2, 128.4, 127.8, 126.7, 126.6, 123.7, 122.9, 122.5, 119.8, 115.7, 115.1, 114.9, 113.4, 55.9. HRMS (ESI-MS) Calc. for $C_{22}H_{18}NO_2S$ $[M+H]^+$, 359.0975; found 359.0975.

(*E*)-1-(10*H*-Phenothiazine-2-yl)-3-(2,3,4-trimethoxyphenyl)-prop-2-en-1-one (FS5)

Dark violet solid. Yield: 26.5 %. Melting point (m.p.): 174.6–175.4 °C. ^{1}H NMR (DMSO-d_6, δ ppm, 400 MHz): 8.77 (s, 1H, NH), 7.82 (d, $J = 15.7$ Hz, 1H, Hß), 7.66 (d, $J = 8.8$ Hz, 1H, ArH), 7.61 (d, $J = 15.7$ Hz, 1H, Hα), 7.50 (dd, $J = 8.2$, 1.8 Hz, 1H, ArH), 7.24 (s, 1H, ArH), 7.03 (d, $J = 8.0$ Hz, 1H, ArH), 6.94 (td, $J = 13.6$, 1.6 Hz, 1H, ArH), 6.87 (d, $J = 4.4$ Hz, 2H, ArH), 6.73 (td, $J = 7.2$, 1.2 Hz, 1H, ArH), 6.64 (d, $J = 8.4$ Hz, 1H, ArH), 3.82 (s, 3H, OCH_3), 3.73 (s, 3H, OCH_3), 3.66 (s, 3H, OCH_3). ^{13}C NMR (DMSO-d_6, δ ppm, 100 MHz): 188.8 (C=O), 156.5, 153.8, 142.8, 142.4, 141.8, 139.1, 137.8, 128.7, 127.0, 126.9, 124.2, 124.0, 123.0, 122.9, 121.6, 120.8, 115.9, 115.3, 113.5, 109.1, 62.2, 61.2, 56.7. Calc. for $C_{24}H_{22}NO_4S$ $[M+H]^+$, 420.1264; found 420.1278.

(*E*)-1-(10*H*-Phenothiazine-2-yl)-3-(2,4,5-trimethoxyphenyl)-prop-2-en-1-one (FS6)

Red solid. Yield: 55.3 %. Melting point (m.p.): 212.2–214.2 °C. ^{1}H NMR (DMSO-d_6, δ ppm, 300 MHz): 8.79 (s, 1H, NH), 8.02 (d, $J = 15.6$ Hz, 1H, Hß), 7.63 (d, $J = 15.5$ Hz, 1H, Hα), 7.58 (d, $J = 1.7$ Hz, 1H, ArH), 7.48 (s, 1H, ArH), 7.29 (d, $J = 1.7$ Hz, 1H, ArH), 7.06 (d, $J = 8.0$ Hz, 1H, ArH), 7.00 (td, $J = 7.7$, 1.4 Hz, 1H, ArH), 6.91 (dd, $J = 7.7$, 1.3 Hz, 1H, ArH), 6.79–6.73 (m, 2H, ArH), 6.67 (dd, $J = 7.9$, 1.0 Hz, 1H, ArH), 3.88 (d, $J = 8.6$ Hz, 6H, OCH_3), 3.81 (s, 3H, OCH_3). ^{13}C NMR (DMSO-d_6, δ ppm, 75 MHz): 188.4 (C=O), 154.8, 153.3, 143.5, 142.6, 141.7, 138.9, 137.9, 128.4, 126.7, 126.5, 123.5, 122.8, 122.5, 119.0, 115.8, 115.1, 114.7, 113.4, 111.5, 98.0, 56.9, 56.3. Calc. for $C_{24}H_{22}NO_4S$ $[M+H]^+$, 419.1186; found 419.1187.

(*E*)-1-(10*H*-Phenothiazine-2-yl)-3-(2,4-dimethoxyphenyl)-prop-2-en-1-one (FS7)

(Do et al. 2016) Red solid. Yield: 28.3 % (49 %, Do et al. 2016). Melting point (m.p.): 189.2–190.4 °C. ^{1}H NMR (DMSO-d_6, δ ppm, 400 MHz): 8.76 (s, 1H, NH), 7.92 (d, J = 15.7 Hz, 1H, Hß), 7.84 (d, J = 8.8 Hz, 1H, ArH), 7.59 (d, J = 15.7 Hz, 1H, Hα), 7.51 (dd, J = 8.1, 1.8 Hz, 1H, ArH), 7.26 (s, 1H, ArH), 7.03 (d, J = 8.1 Hz, 1H, ArH), 7.00–6.96 (m, 1H, ArH), 6.89 (d, J = 7.7 Hz, 1H, ArH), 6.74 (t, 7.5 Hz, 1H, ArH), 6.65–6.59 (m, 3H, ArH), 3.88 (s, 3H, OCH_3), 3.81 (s, 3H, OCH_3). ^{13}C NMR (DMSO-d_6, δ ppm, 100 MHz): 188.6 (C=O), 163.8, 160.7, 142.8, 141.9, 139.3, 138.0, 130.8, 128.7, 127.0, 126.8, 123.7, 122.9, 122.8, 119.5, 116.6, 116.0, 115.9, 113.6, 107.1, 99.0, 56.5, 56.2. Calc. for $C_{23}H_{20}NO_3S$ $[M+H]^+$, 390.1158; found 390.1154.

(*E*)-1-(10*H*-Phenothiazine-2-yl)-3-(2,3-dimethoxyphenyl)-prop-2-en-1-one (FS9)

Claret red solid. Yield: 62.4 %. Melting point (m.p.): 180.1–181.3 °C. ^{1}H NMR (DMSO-d_6, δ ppm, 400 MHz): 8.77 (s,

1H, NH), 7.90 (d, $J = 15.7$ Hz, 1H, Hß), 7.68 (d, $J = 15.7$ Hz, 1H, Hα), 7.53–7.50 (m, 2H, ArH), 7.25 (s, 1H, ArH), 7.11–6.96 (m, 4H, ArH), 6.85 (d, $J = 1.5$ Hz, 1H, ArH), 6.72–6.64 (m, 1H, ArH), 6.62 (d, $J = 1.1$ Hz, 1H, ArH), 3.78 (s, 3H, OCH_3), 3.74 (s, 3H, OCH_3). ^{13}C NMR (DMSO-d_6, δ ppm, 100 MHz): 188.8 (C=O), 153.4, 148.9, 142.8, 141.7,138.6, 137.5, 128.8, 128.7, 126.9, 125.1, 124.4, 123.2, 122.9, 119.7, 115.9, 115.6, 115.3, 113.5, 61.7, 56.4. Calc. for $C_{23}H_{20}NO_3S$ $[M+H]^+$, 390.1158; found 390.1152.

(*E*)-1-(10*H*-Phenothiazine-2-yl)-3-(3,4-dimethoxyphenyl)-prop-2-en-1-one (FS10)

Red solid. Yield: 32.1 %. Melting point (m.p.): 181.6–183.4 °C. ^1H NMR (DMSO-d_6, δ ppm, 400 MHz): 8.78 (s, 1H, NH), 7.66 (s, 2H, ArH), 7.60 (dd, $J = 8.1$, 1.5 Hz, 1H, ArH), 7.49 (s, 1H,ArH), 7.35 (d, $J = 1.5$ Hz, 1H, ArH), 7.33 (s, 1H, ArH) 7.28 (d, $J = 1.5$ Hz, 1H, ArH), 7.07–6.96 (m, 2H, ArH), 6.90 (d, $J = 7.7$ Hz, 1H, ArH), 6.74 (t, $J = 7.5$ Hz, 1H, ArH), 6.65 (d, $J = 7.7$ Hz, 1H, ArH), 3.79 (s, 3H, OCH_3), 3.33 (s, 3H, OCH_3). ^{13}C NMR (DMSO-d_6, δ ppm, 100 MHz): 188.6 (C=O), 152.0, 149.7, 145.1, 142.8, 141.9, 137.9, 128.7, 128.2, 127.0, 126.7, 124.6, 123.9, 123.2, 122.8, 120.1, 115.9, 115.3, 113.6, 112.2, 111.4, 56.4, 56.3. Calc. for $C_{23}H_{20}NO_3S$ $[M+H]^+$, 390.1158; found 390.1159.

(*E*)-1-(10*H*-Phenothiazine-2-yl)-3-(2,5-dimethoxyphenyl)-prop-2-en-1-one (FS11)

Dark violet solid. Yield: 26.6 %. Melting point (m.p.): 205.5–206.4 °C. ^1H NMR (DMSO-d_6, δ ppm, 300 MHz): 8.79 (s, 1H, NH), 7.99 (d, $J = 15.8$ Hz, 1H, Hß), 7.77 (d, $J = 15.8$ Hz, 1H, Hα), 7.61 (dd, $J = 8.1$, 1.8 Hz, 1H, ArH), 7.50 (brs, 1H, ArH), 7.30 (d, $J = 1.7$ Hz, 1H, ArH), 7.07 (d, $J = 8.0$ Hz, 1H, ArH), 7.04–7.02 (m, 2H, ArH), 6.99 (dd, $J = 7.1$, 0.9 Hz, 1H, ArH), 6.91 (dd, $J = 7.7$ Hz, 1.4 Hz, 1H, ArH), 6.79–6.76 (m, 1H, ArH), 6.66 (dd, $J = 7.9$, 1.1 Hz, 1H, ArH), 3.84 (s, 3H, OCH_3), 3.79 (s, 3H, OCH_3). ^{13}C NMR (DMSO-d_6, δ ppm, 75 MHz): 188.5 (C=O), 153.7, 153.2, 142.6, 141.6, 138.6, 137.5, 128.5, 126.7, 126.6, 124.0, 123.0, 122.6, 122.3, 118.6, 115.7, 115.1, 113.5, 113.4, 113.1, 56.6, 56.2. Calc. for $C_{23}H_{20}NO_3S$ $[M+H]^+$, 389.1080; found 389.1082.

Cytotoxic activity

Materials

The following chemicals and reagents were obtained from the indicated companies: Dulbecco's modified Eagle's medium (DMEM) from GIBCO BRL, Grand Island, NY, USA; fetal bovine serum (FBS), 3-(4,5-dimethylthiazol-2-yl)-2,5-diphenyltetrazolium bromide (MTT), doxorubicin, and dimethyl sulfoxide (DMSO) from Wako Pure Chem. Ind., Osaka, Japan; and culture plastic dishes and plates (96-well) were purchased from Becton Dickinson (Franklin Lakes, NJ, USA).

Cell culture

Human normal oral mesenchymal cells, gingival fibroblast (HGF), periodontal ligament fibroblast (HPLF), and pulp cell (HPC) established from the first premolar tooth extracted from the lower jaw of a 12-year-old girl (Kantoh et al. 2010), and human OSCC cell line Ca9-22 (derived from gingiva), HSC-2, HSC-3, and HSC-4 (derived from tongue), purchased from Riken Cell Bank (Tsukuba, Japan), were cultured at 37 °C in DMEM supplemented with 10% heat-inactivated FBS, 100 units/ml penicillin G and 100 µg/ml streptomycin sulfate under a humidified 5% CO_2 atmosphere. HGF, HPLF, and HPC cells at 10–18 population doubling levels were used in the present study.

Assay for cytotoxic activity

Cells were inoculated at 2.5×10^3 cells/0.1 ml in a 96-microwell plate (Becton Dickinson Labware, Franklin Lakes, NJ, U.S.A.). After 48 h, the medium was replaced with 0.1 ml of fresh medium containing different concentrations of single test compounds. Cells were incubated further for 48 h and the relative viable cell number was then determined by the MTT (3-(4,5-Dimethylthiazol-2-yl)-2,5-diphenyltetrazolium bromide) method (Yerdelen et al. 2015; Yamali et al. 2016, 2017a; Unluer et al. 2016; Tugrak et al. 2016; Sakagami et al. 2017a; Gul et al. 2016a, 2016b, 2017a, 2017b, 2018; Yamali et al. 2017b). All phenothiazine derivatives were dissolved with DMSO at the concentration of 40 mM and stored until use. Control cells were treated with the same amounts of DMSO (0.00156, 0.03125, 0.0625, 0.125, 0.25, 0.5, 1.0%) and the cell damage induced by DMSO was subtracted from that induced by test agents. In brief, cells were stained with MTT reagent, dissolved with DMSO, and the absorbance of the MTT-stained cell lysate was measured at 560 nm, using a microplate reader (Infinite F 50 R, TECAN, Kawasaki, Japan). Control cells were treated with the same amounts of DMSO and the cell damage induced by DMSO was subtracted from that induced by test agents. The concentration of compound that reduced the viable cell number by 50% (CC_{50}) was determined from the dose-response curve and the mean value of CC_{50} for each cell type was calculated from triplicate assays.

Calculation of tumor specificity

Tumor specificity (TS) was calculated using the following equation: TS = Mean CC_{50} against three normal oral cell types (HGF, HPLF, HPC)/Mean CC_{50} against four OSCC cell lines (Ca9-22, HSC-2, HSC-3, HSC-4). Since both Ca9-22 and HGF cells were derived from gingival tissue (Horikoshi et al. 1974), the relative sensitivity of these cells was also compared (as: mean CC_{50} against HGF/mean CC_{50} against Ca9-22).

Calculation of potency-selectivity expression

Potency-selectivity expression (PSE) was calculated by the following equation: PSE = Mean CC_{50} against three normal oral cell types/(CC_{50} against four OSCC cell lines)$^2 \times 100$ (HGF, HPLF, HPC vs. Ca9-22, HSC-2, HSC-3, HSC-4); and as mean CC_{50} against HGF/(CC_{50} against Ca9-22)$^2 \times 100$ using the pair of cell types from the same tissue (gingiva).

Western blot analysis

The cells were washed with phosphate buffer solution (PBS) and processed for western blot analysis, as described previously (Sakagami et al. 2017b). Antibodies against cleaved caspase-3 (Cell Signaling Technology Inc., Beverly, MP, USA), poly(ADP-ribose) polymerase (PARP) (Cell Signaling Technology Inc.) and glyceraldehyde 3-phosphate dehydrogenase (GAPDH; Trevigen, Gaithersburg, MD, USA) were used as primary antibodies. α-Rabbit IgG (DAKO Japan) antibodies, which were conjugated with horseradish peroxidase, were used as secondary antibodies.

Computational analysis

Estimation of CC_{50} values

Since the CC_{50} values had a distribution pattern close to a logarithmic normal distribution, we used the pCC_{50} (i.e, the $-\log CC_{50}$) for the comparison of the cytotoxicity between the compounds. The mean pCC_{50} values for normal cells and tumor cell lines were defined as N and T, respectively.

Calculation of chemical descriptor

The 3D structure of each chemical structure (drawn by Marvin) was optimized by CORINA Classic (Molecular Networks GmbH, Germany) with partial charge calculations (Amber-10: EHT) in Molecular Operating Environment (MOE) version 2015.1001 (Chemical Computing Group Inc., Quebec, Canada). The number of structural descriptors calculated from MOE and Dragon 7.0 (Kode srl., Pisa, Italy) after the elimination of overlapped descriptors were 278 and 2714, respectively. The following eleven Dragon descriptors (Complete list of descriptors calculated by Dragon 7, https://chm.kode-solutions.net/products_dragon_descriptors.php), Dipole moment, and three vsurf descriptors (Cruciani et al. 2000) were significantly correlated with T, N, and T-N (Table 1). Dragon descriptors: Eig03_AEA and Eig03_EA (Eigenvalue from augmented edge adjacency matrix), HATS6m (Leverage-weighted autocorrelation of lag 6/weighted by mass in GETAWAY descriptors), Mor18m (Signal 18/weighted by mass in 3D-MoRSE descriptors), R2 (R maximal autocorrelation of lag 2 in GETAWAY descriptors), SM11_AEA (Spectral moment of order 11 from augmented edge adjacency matrix), VE1sign_Dz (Coefficient sum of the last eigenvector from Barysz matrix in 2D matrix-based descriptors). MOE descriptors: Dipole (Dipole moment), vsurf_CW6 (Capacity factor 6), vsurf_D6 (Hydrophobic volume 6), vsurf_W6 (Hydrophilic volume 6).

Statistical treatment

The relation among cytotoxicity and TS index with chemical descriptors was investigated using simple regression analyses by JMP Pro version 12.2.0 (SAS Institute Inc., Cary, NC, USA). The significance level was set at $p < 0.05$.

Results and discussion

Chemistry

Chalcones having the chemical structure of (*E*)-1-(10*H*-phenothiazine-2-yl)-3-aryl-prop-2-en-1-ones **FS1–11**, were successfully synthesized according to Scheme 1. The compounds designed were prepared by the reaction of 2-acetylphenothiazine with a suitable benzaldehyde via base-catalyzed Claisen–Schmidt condensation. Aryl part was changed as phenyl (**FS1**), 2-methoxyphenyl (**FS2**), 3,4,5-trimethoxyphenyl (**FS3**), 4-methoxyphenyl (**FS4**), 2,3,4-trimethoxyphenyl (**FS5**), 2,4,5-trimethoxyphenyl (**FS6**), 2,4-dimethoxyphenyl (**FS7**), 2,3-dimethoxyphenyl (**FS9**), 3,4-dimethoxyphenyl (**FS10**), and 2,5-dimethoxyphenyl (**FS11**). The compound 2,4,6-trimethoxyphenyl (**FS8**) derivative was synthesized but it was not purified sufficiently by crystallization and/or column chromatography. The compounds **FS3**, **FS5**, **FS6**, **FS9**, and **FS11** were reported here for the first time, i.e., they are original compounds. Other registered compounds were reported with several bioactivities such as antifungal, antimicrobial, antioxidant, and cytotoxic activities or they were used in chemical reactions as intermediate compounds in several

Table 1 Explanation of chemical descriptors that correlate with cytotoxicity to tumor cells, normal cells and tumor specificity

Descriptor	Source	Explanation
Eig03_AEA(bo)	Dragon	Eigenvalue n. 3 from augmented edge adjacency mat. weighted by bond order in Edge adjacency indices
Eig03_AEA(ri)	Dragon	Eigenvalue n. 3 from augmented edge adjacency mat. weighted by resonance integral in Edge adjacency indices
Eig03_EA	Dragon	Eigenvalue n. 3 from edge adjacency matrix in Edge adjacency indices
Eig03_EA(ri)	Dragon	Eigenvalue n. 3 from edge adjacency mat. weighted by resonance integral in Edge adjacency indices
HATS6m	Dragon	Leverage-weighted autocorrelation of lag 6/weighted by mass in GETAWAY descriptors
Mor18m	Dragon	Signal 18 / weighted by mass in 3D-MoRSE descriptors
R2e+	Dragon	R maximal autocorrelation of lag 2/weighted by Sanderson electronegativity in GETAWAY descriptors
R2i+	Dragon	R maximal autocorrelation of lag 2/weighted by ionization potential in GETAWAY descriptors
R2u+	Dragon	R maximal autocorrelation of lag 2/unweighted in GETAWAY descriptors
SM11_AEA(bo)	Dragon	Spectral moment of order 11 from augmented edge adjacency mat. weighted by bond order in Edge adjacency indices
VE1sign_Dz(v)	Dragon	Coefficient sum of the last eigenvector from Barysz matrix weighted by van der Waals volume in 2D matrix-based descriptors
Dipole	MOE	Dipole moment calculated from the partial charges of the molecule
vsurf_CW6	MOE	Capacity factor 6 in the vsurf_ descriptors which are similar to the VolSurf descriptors
vsurf_D6	MOE	Hydrophobic volume 6 in the vsurf_ descriptors which are similar to the VolSurf descriptors
vsurf_W6	MOE	Hydrophilic volume 6 in the vsurf_ descriptors which are similar to the VolSurf descriptors

Dragon, Complete list of descriptors calculated by Dragon 7, https://chm.kode-solutions.net/products_dragon_descriptors.php; vsurf_CW6, vsurf_D6, and vsurf_W6 (Cruciani et al. 2000)

studies (Do et al. 2016; Ranganathan et al. 2013; Saranya and Ravi 2014; Bansode and Meshram 2012). The chemical structure of the compounds **FS1-FS11** were confirmed according to spectral techniques, such as ^{1}H NMR, ^{13}C NMR, and HRMS. The compounds synthesized in this study were seen as *E* isomer on the basis of coupling constants (*J*) around 15 Hz. A signal belong to N-H group on phenothiazine ring was observed 8.79–8.76 ppm as a singlet. In ^{13}C NMR, a signal of carbonyl group was seen around 188 ppm.

Cytotoxicity and tumor specificity

As mentioned previously in introduction section, several phenothiazines, and/or chalcones had potent anticancer/cytotoxic activities with different mechanisms of action (Yerdelen et al. 2015; Yde et al. 2009; Yamali et al. 2017a; Varga et al. 2017; Unluer et al. 2016; Singh et al. 2014; Raghavendra et al. 2018; Pluta et al. 2011; Mahapatra et al. 2015; Gomes et al. 2017; Ghinet et al. 2016; Fond et al. 2012; Do et al. 2016; Yamali et al. 2017b).

Similarly, in this study, the designed compounds bearing chalcone and tricyclic phenothiazine pharmacophores were evaluated in terms of their anticancer/cytotoxic effects on several cancer cell lines. Chalcones (**FS1-FS11**) were screened for their *in vitro* cytotoxic effects against four human OSCC cell lines (Ca9-22, HSC-2, HSC-3, and HSC-4) and three human normal oral cells (HGF, HPLF, HPC) by MTT test. Doxorubicin was used as a reference drug in MTT test.

All compounds showed relatively higher cytotoxicity against four human OSCC cell lines (Ca9-22, HSC-2, HSC-3, and HSC-4) over three human normal oral cells (HGF, HPLF, HPC) (Table 2). The CC_{50} values of the compounds are in the range of 0.9–109.8 μM towards OSCC malign cell lines while the reference drug doxorubicin had CC_{50} values between 0.1–0.3 μM. The conclusion to be drawn is that chalcones possess antineoplastic potencies.

Selectivity is the main problem of the drugs in clinical use for the cancer treatment. If the compound has more selectivity potency towards cancer cells than normal cells, that compound can be evaluated as anticancer drug candidate for further research. In order to quantify the greater cytotoxicity for malign cell lines than nonmalignant cells, selectivity index (SI) values were calculated. SI values are the quotients of the average CC_{50} values towards HGF, HPLF, and HPC cells and the CC_{50} values of the compound against a specific malign cell line. If the average SI value of the compound is higher than 1, that compound can be considered as a selective cytotoxic compound (Yerdelen et al. 2015; Yamali et al. 2016, 2017a; Tugrak et al. 2016; Robles-Escajeda et al. 2016; Gul et al. 2016a, 2016b, 2017a; Yamali et al. 2017b). The SI values of the compounds are presented in Table 2. According to average SI value of the compounds, all compounds showed high SI values in the range of 1.8–76.5. The compound **FS6** bearing 2,4,5-trimethoxyphenyl had the greatest selectivity with the highest SI value 76.5.

TS was calculated for the compounds by dividing the average CC_{50} value towards normal cells to the average

Table 2 Cytotoxic activity of the compounds **FS1–11** against oral malignant and nonmalignant cells

	CC_{50} (μM)								
	Human normal oral cells				TS			PSE	
Compound	(C) HGF	HPLF	HPC	(D) Mean	SD	D/B	C/A	(D/B^2) ×100	(C/A^2) ×100
FS1	>400	>400	>400	400.0	0.0	>8.8	>16.3	>19	>67
FS2	18.2	50.3	129.3	65.9	57.2	19.7	5.5	588	164
FS3	4.4	6.2	8.8	6.5	2.2	3.7	2.9	217	194
FS4	9.8	13.3	24.2	15.8	7.5	1.6	0.7	16	4
FS5	15.2	26.2	95.2	45.5	43.3	8.7	4.6	166	137
FS6	131.7	>400	>400	310.6	154.9	>63.2	>45.9	>1285	>1602
FS7	22.7	37.8	130.7	63.7	58.5	33.4	23.5	1749	2429
FS9	10.4	17.9	16.6	15.0	4.0	5.7	6.7	218	425
FS10	21.8	33.3	66.8	40.6	23.4	12.4	14.2	381	927
FS11	8.3	11.2	18.0	12.5	5.0	5.3	6.7	227	543
DXR	1.0	9.2	10.0	6.7	5.0	39.0	2.8	22721	799

	CC_{50} (μM)										
	Human oral squamous cell carcinoma cell lines										
Compound	(A) Ca9-22	SI	HSC-2	SI	HSC-3	SI	HSC-4	SI	(E) SI Mean	(B) CC_{50} Mean	SD
FS1	24.5	16.3	38.2	10.5	9.8	41.0	109.8	3.6	17.8	45.6	44.4
FS2	3.3	19.8	4.3	15.2	1.4	47.1	4.3	15.2	24.3	3.4	1.4
FS3	1.5	4.3	2.7	2.4	0.9	7.2	1.8	3.6	4.4	1.7	0.8
FS4	14.8	1.1	10.2	1.6	5.8	2.7	9.4	1.7	1.8	10.0	3.7
FS5	3.3	13.7	6.4	7.1	4.1	11.2	7.1	6.4	9.6	5.2	1.8
FS6	2.9	108.3	8.4	37.1	3.0	103.5	5.4	57.2	76.5	4.9	2.6
FS7	1.0	65.9	2.4	26.2	1.4	44.4	2.8	22.8	39.8	1.9	0.9
FS9	1.6	9.6	2.8	5.4	2.1	7.0	4.0	3.7	6.4	2.6	1.0
FS10	1.5	26.5	3.1	13.0	2.5	16.0	5.9	6.9	15.6	3.3	1.9
FS11	1.2	10.1	2.9	4.3	2.4	5.1	2.8	4.5	6.0	2.3	0.8
DXR	0.3	19.4	0.1	57.5	0.1	54.4	0.1	66.6	49.5	0.2	0.1

Each value represents the mean ± S.D. of triplicate determinations. The compound FS8 was not purified sufficiently and therefore was not used for the experiment

HGF human gingival fibroblast, *HPLF* human periodontal ligament fibroblast, *HPC* human pulp cell, *Ca9-22, HSC-2, HSC-3, and HSC-4* oral squamous cell carcinoma cell lines, *DXR* doxorubicin, *SI* selectivity index, *TS* tumor specificity, *PSE* potency-selectivity expression, *CC_{50}* 50% cytotoxic concentration, *SD* standart deviation

CC_{50} value towards cancer cell lines. (Column D/Column B, Table 2). Among them, the compound **FS6** showed the highest TS (TS = >63.2 in Table 2) and **FS6** was superior than that of doxorubicin (TS = 39.0). By considering the fact that HGF is the corresponding normal cell of Ca9-22 cancer cell line having the same origin (both derived from gingival tissues), TS values were also generated for a compound by dividing the CC_{50} value towards HGF cells into the CC_{50} value towards Ca9-22 cell line (Column C/ Column A, Table 2). It reveals that the compound **FS6** showed the highest TS (TS = >45.9 in Table 2), exceeding that of doxorubicin (TS = 2.8).

In order to determine the most promising compounds in terms of both good potencies and selective cytotoxicity, the PSE values were calculated according to equations PSE=TS/CC_{50} against tumor cells × 100 [that is, (Equation 1 = (D/B^2) × 100) (HGF, HPLF, HPC vs. Ca9-22, HSC-2, HSC-3, HSC-4)] and [(Equation 2 = C/A^2) × 100 (HGF vs Ca9-22 in Table 2)]. (Sakagami et al. 2017a, 2017b) PSE values of the compounds were changed in the range of 16-1749 based on the first equation while the PSE values were in the range of 4-2429 based on the second equation. The compounds **FS6**, (*E*)-1-(10*H*-phenothiazine-2-yl)-3-(2,4,5-trimethoxyphenyl)-prop-2-en-1-one, (PSE = >1285 and

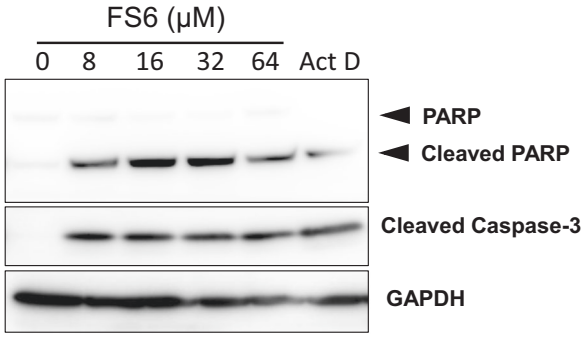

Fig. 4 Induction of apoptosis by **FS6** in HSC-2 cells. HSC-2 cells were incubated for 24 h without (0.16% DMSO) or with 8, 16, 32, or 64 μM of FS6 or with 1 μM actinomycin D (Act D), and subjected to western blot analysis. The results show that 8–64 μM FS6 induced apoptosis (production of a cleaved product of PARP (substrate of caspase-3) and activation of caspase-3 (as evidenced by cleavage into active form). The mean (pCC_{50} i.e., the $-\log CC_{50}$) values for tumor cell lines were defined as T

>1602) and **FS7**, (*E*)-1-(10*H*-phenothiazine-2-yl) -3-(2,4-dimethoxyphenyl)-prop-2-en-1-one, (PSE = 1749 and 2429) had the highest and remarkably impressive PSE values than others.

Apoptosis is a programmed "self-automated" cell death with caspase-3 as a key player in apoptotic process execution (Rudel 1999). It is critical for the homeostasis that conserves cellular integrity. Impairment of apoptosis signaling pathways may lead to several diseases including cancer (Ma et al. 2017). Here we have evaluated the prospects of compound **FS6** as an anticancer drug candidate and investigated how this compound affects apoptosis process. Western blot analysis demonstrated that **FS6** (8–64 μM) induced the production of cleaved product of PARP (substrate of caspase-3) and the activation of caspase-3 (as evidenced by cleavage into active form) in HSC-2, as potently as actinomycin D (ActD), a positive control of apoptosis, suggesting that **FS6** induced apoptosis in HSC-2 cells (Fig. 4).

Structure-activity relationship (SAR) of the compounds

Recently, our research group have reported a set of chalcones containing polymethoxy phenyl group which have valuable selective anticancer activity against human OSCC cell lines (Yamali et al. 2017a, 2017b). The results obtained promted us to design new chalcones bearing mono, di or tri methoxyphenyl groups on its chemical structure to understand which position is favorable for the methoxy groups.

When the substitution pattern was considered, methoxy substitution at ortho position of phenyl increased SI (24.3) and PSE (588 and 164) values for **FS2**, and that at para position decreased the SI (1.8) and PSE (16 and 4) values for **FS4**, comparing with nonsubstituted derivative **FS1**'s [SI (17.8) and PSE (>19 and >67)].

When the dimethoxy substituted derivatives (**FS7**, **FS9**, **FS10**, **FS11**) were considered in their series, 2,4-dimethoxy derivative **FS7** and 3,4-dimethoxy derivative **FS10** were more selectively cytotoxic than others with the highest SI (**TP7** = 39.8, **TP10** = 15.6) and PSE (**TP7** = 1749;2429 and **TP10** = 381;927) values. It seems that converting the nonsubstituted derivative **FS1** to dimethoxy substituted derivatives was useful and effective molecular modification based on the CC_{50}, SI, and PSE values.

When cytotoxic effects of the trimethoxy substituted derivatives (**FS3**, **FS5**, **FS6**) were considered, the compound **FS6** with 2,4,5-trimethoxyphenyl was more selective compound among the trimethoxylated derivatives with the highest SI (76.5) and PSE (>1285; >1602) values. When the SI value of **FS6** was compared with **FS1**'s, it was found that **FS6** was 4.3 times more selective than nonsubstituted derivative **FS1**. **FS6** was also found 1.6 times more selective cytotoxic than reference drug doxorubicin according to SI value comparison.

Computational analysis

We next performed the quantitative structure-activity relationship (QSAR) analysis of **FS 1-11** derivatives in regards to their cytotoxicity against four human OSCC cells and three human normal oral cells. Among a total of 2992 descriptors (2714 Dragon descriptors and 278 MOE descriptors), 15 descriptors described below correlated well with cytotoxicity and TS.

Cytotoxicity of **FS** derivatives against human tumor cells (T) was correlated with SM11_AEA (bo) ($r^2 = 0.830$, $p = 0.0002$), Eig03_EA ($r^2 = 0.830$, $p = 0.0002$), Eig03_AEA (bo) ($r^2 = 0.828$, $p = 0.0003$), Eig03_AEA(ri) ($r^2 = 0.824$, $p = 0.0003$), HATS6m ($r^2 = 0.822$, $p = 0.0003$), and Eig03_EA(ri) ($r^2 = 0.820$, $p = 0.0003$) (Fig. 5). These descriptors represent topological shapes with molecular properties such as bound order, resonance integral, and atomic weight.

Cytotoxicity of **FS** derivatives against human normal cells (N) was correlated with R2u + ($r^2 = 0.774$, $p = 0.0008$), R2i + ($r^2 = 0.768$, $p = 0.00029$), R2e + ($r^2 = 0.753$, $p = 0.0011$), dipole ($r^2 = 0.752$, $p = 0.0012$), Mor18m ($r^2 = 0.584$, $p = 0.0101$), and VE1sign_Dz(v) ($r^2 = 0.565$, $p = 0.0122$) (Fig. 6). R2u +, R2i +, R2e +, and VE1sign_Dz(v) represent topological shape, shape with ionization potential, shape with electronegativity, and shape with atomic volume, respectively. Mor18m and dipole represent molecular shape with atomic weight and dipole moment, respectively.

TS of **FS** derivatives (T-N) was correlated with vsurf_D6 ($r^2 = 0.741$, $p = 0.0014$), R2e + ($r^2 = 0.628$, $p = 0.0062$),

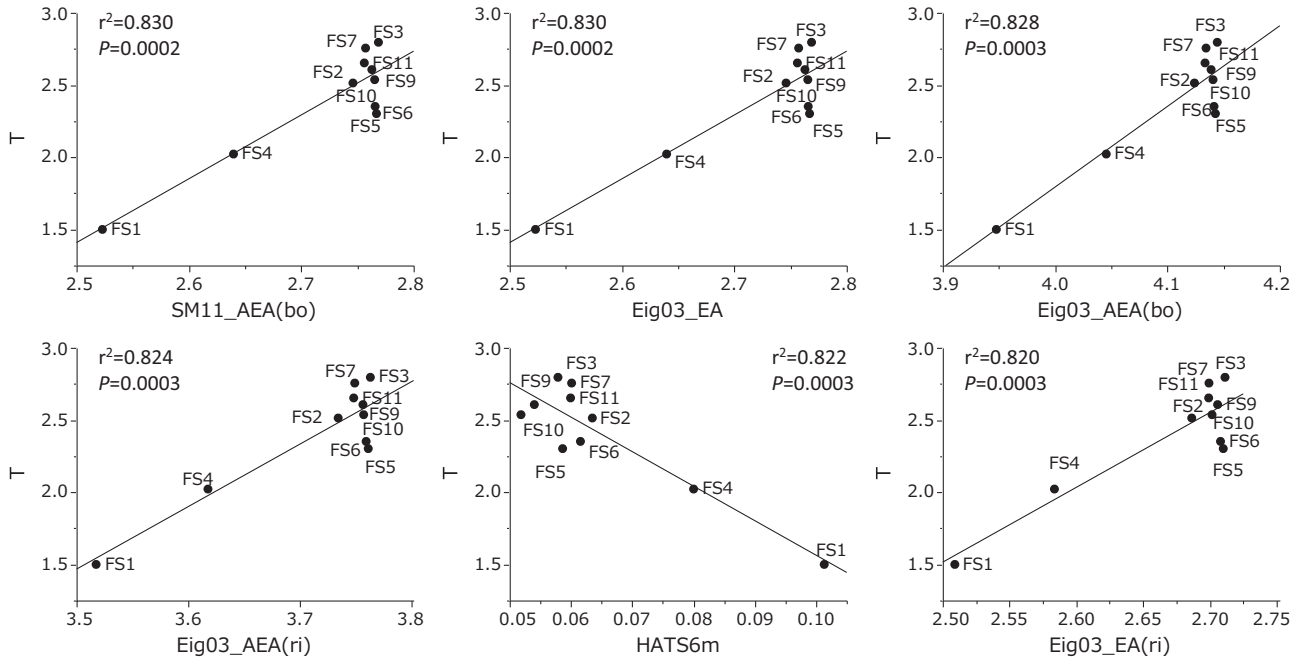

Fig. 5 Determination of coefficient between chemical descriptors and cytotoxicity of **FS** derivatives against tumor cells (defined as T). The mean (pCC_{50} i.e., the $-\log CC_{50}$) values for normal cells were defined as N

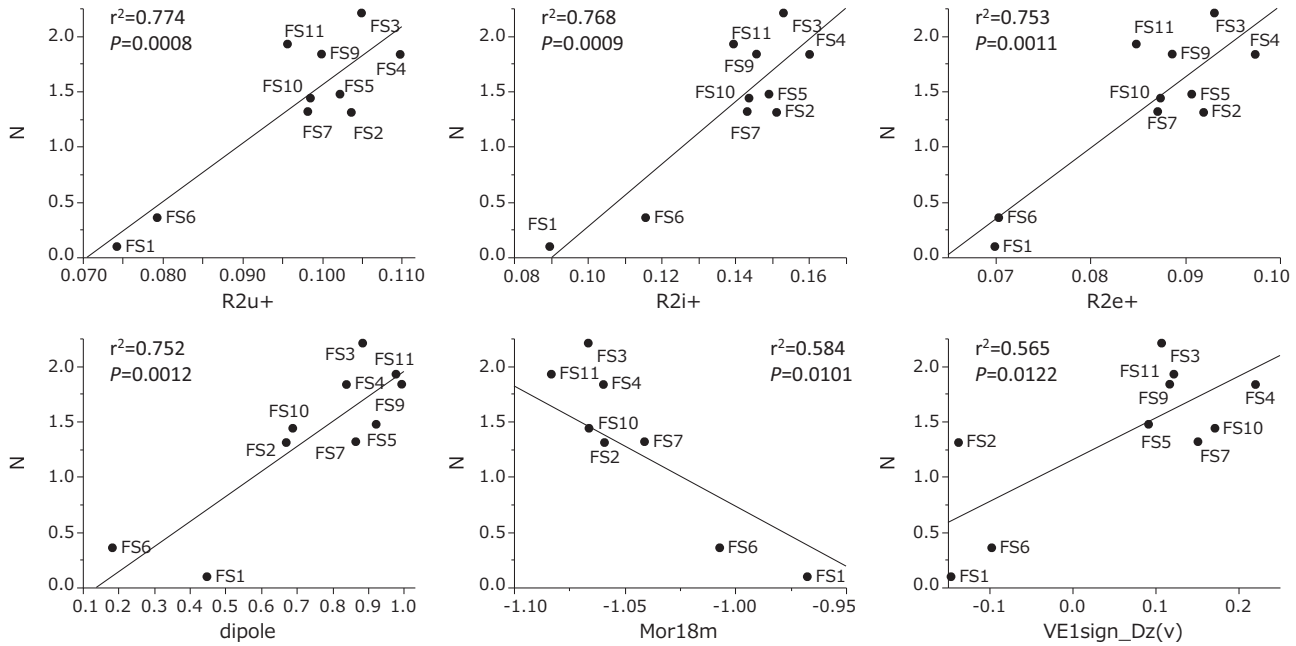

Fig. 6 Determination of coefficient between chemical descriptors and cytotoxicity of **FS** derivatives against normal cells (defined as N)

dipole ($r^2 = 0.607$, $p = 0.0079$), vsurf_CW6 ($r^2 = 0.590$, $p = 0.0095$), R2u + ($r^2 = 0.575$, $p = 0.0110$), and vsurf_W6 ($r^2 = 0.538$, $p = 0.0158$) (Fig. 7). vsurf_D6, vsurf_CW6, and vsurf_W6 represent hydrophobic volume, capacity factor, and hydrophilic volume, respectively. R2u + and R2e + represent topological shape and shape convoluted with electronegativity, respectively. Dipole means dipole moment.

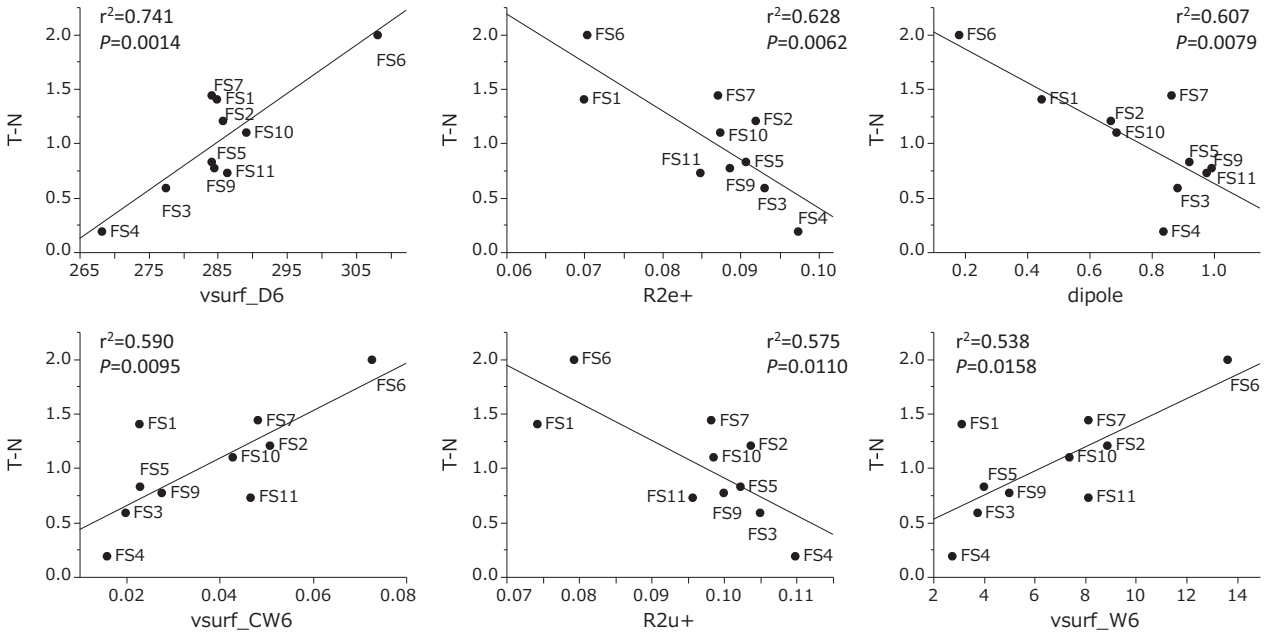

Fig. 7 Determination of coefficient between chemical descriptors and tumor specificity of **FS** derivatives (defined as T−N)

Bicyclic chromene derivatives were reported as highly tumor-specific compounds in our previous studies as mentioned below. Their TS was well correlated with: molecular shape and electrostatic interaction (3-styrylchromone derivatives) (Shimada et al. 2014); molecular shape and flatness (3-styryl-2*H*-chromene derivatives) (Uesawa et al. 2015), three dimensional (D) shapes and polarization (3-benzylidenechromanones) (Uesawa et al. 2016), 3D shape, polarizability, ionization potential, and lipophilicity (2-azolylchromones) (Sakagami et al. 2018), the number of intramolecular unsaturated bonds, molecular flexibility, molecular density, lipophilicity, molecular size, and molecular shape (furo[2,3-b]chromones) (Uesawa et al. 2018), molecular shape, especially 3D structure (2-(*N*-cyclicamino) chromone derivatives) (Shi et al. 2018a), 3D structure and lipophilicity (3-(*N*-Cyclicamino)chromone derivatives) (Shi et al. 2018b), and 3D structure, polarity, ionic potential, and electric state (pyrano[4,3-b]chromones) (Nagai et al. 2018). This suggests that molecular shape and hydrophobicity are important factors to increase the TS in addition to the location of substituted groups.

Conclusion

Newly synthesized methoxylated phenothiazine bearing chalcones (*E*)-1-(10*H*-phenothiazine-2-yl)-3-aryl-prop-2-en-1-ones **FS1-11**, were reported here for the first time with their cytotoxicities and their QSAR studies. The compound **FS6**, (*E*)-1-(10*H*-phenothiazine-2-yl)-3-(2,4,5-trimethoxyphenyl)-prop-2-en-1-one, was found to be the most selective cytotoxic compound with the highest SI (76.5) and PSE (> 1285; > 1602) values among the compounds studied. Western blot analysis suggested that **FS6** (8–64 μM) induced apoptosis in HSC-2 cells. QSAR analysis suggested that the TS of the chalcones correlated with their molecular shape, volume, and electrostatic properties. Therefore, **FS6** can be considered as a lead compound for further modifications in designing new anticancer drug candidate compound.

Acknowledgements This study was supported by Ataturk University BAP Office, Project Number is 2016-110 and supported by KAKENHI from the Japan Society for the Promotion of Science (JSPS) (15K08111, 16K11519). The annual license of the statistical software, JMP Pro, was supported by the grant-in-aid of the oncology specialists promotion program by the Ministry of Education, Culture, Sports, Science and Technology, Japan.

Compliance with ethical standards

Conflict of interest The authors declare that they have no conflict of interest.

References

Badr G, Gul HI, Yamali C, Mohamed AAM, Badr BM, Gul M, Markeb AA, El-Maali NA (2018) Curcumin analogue 1,5-bis(4-hydroxy-3-((4-methylpiperazin-1-yl)methyl)phenyl)penta-1,4-dien-3-one mediates growth arrest and apoptosis by targeting the PI3K/AKT/mTOR and PKC-theta signaling pathways in human breast carcinoma cells. Bioorg Chem 78:46–57

Bansode TN, Meshram G (2012) Synthesis and antimicrobial activity of 4-(10*H*-phenothiazin-2-yl)-pyrimidin-2(1H)-one/thione derivatives. J Het Chem 49:1004–1008

Cruciani GCP, Carrupt P-A, Testa B (2000) Molecular fields in quantitative structure-permeation relationships: the VolSurf Approach. J Mol Struct (Theochem) 503:17–30

Das U, Gul HI, Alcorn J, Shrivastav A, George T, Sharma RK, Nienaber KH, De Clercq E, Balzarini J, Kawase M, Kan N, Tanaka T, Tani S, Werbovetz KA, Yakovich AJ, Manavathu EK, Stables JP, Dimmock JR (2006) Cytotoxic 5-aryl-1-(4-nitrophenyl)-3-oxo-1,4-pentadienes mounted on alicyclic scaffolds. Eur J Med Chem 41:577–585

Do TH, Nguyen DM, Truong VD, Do TH, Le MT, Pham TQ, Thai KM, Tran TD (2016) Synthesis and selective cytotoxic activities on rhabdomyosarcoma and noncancerous cells of some heterocyclic chalcones. Molecules 21:329

Eriksson A, Yachnin J, Lewensohn R, Nilsson A (2001) DNA-dependent protein kinase is inhibited by trifluoperazine. Biochem Biophys Res Commun 283:726–731

Fond G, Macgregor A, Attal J, Larue A, Brittner M, Ducasse D, Capdevielle D (2012) Antipsychotic drugs: pro-cancer or anti-cancer? A systematic review. Med Hypotheses 79:38–42

Ghinet A, Moise IM, Rigo B, Homerin G, Farce A, Dubois J, Bicu E (2016) Studies on phenothiazines: new microtubule-interacting compounds with phenothiazine A-ring as potent antineoplastic agents. Bioorg Med Chem 24:2307–2317

Gomes MN, Muratov EN, Pereira M, Peixoto JC, Rosseto LP, Cravo PVL, Andrade CH, Neves BJ (2017) Chalcone derivatives: promising starting points for drug design. Molecules 22:1210–1235

Gul HI, Cizmecioglu M, Zencir S, Gul M, Canturk P, Atalay M, Topcu Z (2009) Cytotoxic activity of 4′-hydroxychalcone derivatives against Jurkat cells and their effects on mammalian DNA topoisomerase I. J Enzym Inhib Med Chem 24:804–807

Gul HI, Mete E, Eren SE, Sakagami H, Yamali C, Supuran CT (2017a) Designing, synthesis and bioactivities of 4-[3-(4-hydroxyphenyl)-5-aryl-4,5-dihydro-pyrazol-1-yl]benzenesulfonamides. J Enzym Inhib Med Chem 32:169–175

Gul HI, Tugrak M, Sakagami H (2016a) Synthesis of some acrylophenones with N-methylpiperazine and evaluation of their cytotoxicities. J Enzym Inhib Med Chem 31:147–151

Gul HI, Tugrak M, Sakagami H, Taslimi P, Gulcin I, Supuran CT (2016b) Synthesis and bioactivity studies on new 4-(3-(4-substitutedphenyl)-3a,4-dihydro-3*H*-indeno[1,2-c]pyrazol-2-yl) benzenesulfonamides. J Enzym Inhib Med Chem 31:1619–1624

Gul HI, Yamali C, Yesilyurt F, Sakagami H, Kucukoglu K, Gulcin I, Gul M, Supuran CT (2017b) Microwave-assisted synthesis and bioevaluation of new sulfonamides. J Enzym Inhib Med Chem 32:369–374

Gul HI, Yerdelen KO, Das U, Gul M, Pandit B, Li PK, Dimmock JR (2008) Synthesis and cytotoxicity of novel 3-aryl-1-(3′-dibenzylaminomethyl-4′-hydroxyphenyl)-propenones and related compounds. Chem Pharm Bull (Tokyo) 56:1675–1681

Gul HI, Yerdelen KO, Gul M, Das U, Pandit B, Li PK, Secen H, Sahin F (2007) Synthesis of 4′-hydroxy-3′-piperidinomethylchalcone derivatives and their cytotoxicity against PC-3 cell lines. Arch Pharm (Weinh) 340:195–201

Gul HI, Yamali C, Sakagami H, Angeli A, Leitans J, Kazaks A, Tars K, Ozgun DO, Supuran CT (2018) New anticancer drug candidates sulfonamides as selective hCA IX or hCA XII inhibitors. Bioorg Chem 77:411–419

Horikoshi M, Kimura Y, Nagura H, Ono T, Ito H (1974) A new human cell line derived from human carcinoma of the gingiva. I. Its establishment and morphological studies. Jpn J Oral Maxillofac Surg 20:100–106

Kantoh K, Ono M, Nakamura Y, Nakamura Y, Hashimoto K, Sakagami H, Wakabayashi H (2010) Hormetic and anti-radiation effects of tropolone-related compounds. In Vivo 24:843–851

Ma Y, Wei X, Wu Z (2017) HNF-4alpha promotes multidrug resistance of gastric cancer cells through the modulation of cell apoptosis. Oncol Lett 14:6477–6484

Mahapatra DK, Bharti SK, Asati V (2015) Anti-cancer chalcones: structural and molecular target perspectives. Eur J Med Chem 98:69–114

Meunier B (2008) Hybrid molecules with a dual mode of action: dream or reality? Acc Chem Res 41:69–77

Nagai J, Shi H, Kubota Y, Bandow K, Okudaira N, Uesawa Y, Sakagami H, Tomomura M, Tomomura A, Takao K, Sugita Y (2018) Quantitative structure–cytotoxicity relationship of pyrano[4,3-b]chromones Anticancer Res 38(8):4449–4457

Ohlow MJ, Moosmann B (2011) Phenothiazine: the seven lives of pharmacology's first lead structure. Drug Discov Today 16:119–131

Pluta K, Morak-Mlodawska B, Jelen M (2011) Recent progress in biological activities of synthesized phenothiazines. Eur J Med Chem 46:3179–3189

Raghavendra NM, Pingili D, Kadasi S, Mettu A, Prasad S (2018) Dual or multi-targeting inhibitors: the next generation anticancer agents. Eur J Med Chem 143:1277–1300

Ranganathan K, Suresh R, Kamalakkannan D (2013) Electrochemical reduction potential correlation of some insect antifeedant potent 2-phenothiazinyl chalcones. Int Lett Chem, Phys Astron 4:66–75

Robles-Escajeda E, Das U, Ortega NM, Parra K, Francia G, Dimmock JR, Varela-Ramirez A, Aguilera RJ (2016) A novel curcumin-like dienone induces apoptosis in triple-negative breast cancer cells Cell Oncol (Dordr) 39:265–277

Rudel T (1999) Caspase inhibitors in prevention of apoptosis. Herz 24:236–241

Sakagami H, Uesawa Y, Masuda Y, Tomomura M, Yokose S, Miyashiro T, Murai J, Takao K, Kanamoto T, Terakubo S, Kagaya H, Nakashima H, Sugita Y (2017a) Quantitative structure-cytotoxicity relationship of newly synthesized piperic acid esters. Anticancer Res 37:6161–6168

Sakagami H, Okudaira N, Masuda Y, Amano O, Yokose S, Kanda Y, Suguro M, Natori T, Oizumi H, Oizumi T (2017b) Induction of apoptosis in human oral keratinocyte by doxorubicin. Anticancer Res 37:1023–1029

Sakagami H, Okudaira N, Uesawa Y, Takao K, Kagaya H, Sugita Y (2018) Quantitative structure-cytotoxicity relationship of 2-azolylchromones. Anticancer Res 38:763–770. PMID: 29374700

Saranya AV, Ravi S (2013) In vitro antifungal activity of chalcones with phenothiazine ring. Int J OrgBioorg Chem 3(2):9–12

Saranya AV, Ravi S (2014) Synthesis of 5-phenyl-3-(10H-phenothiazinyl)-Δ2-cyclohexen-1-ones by conventional and microwave assisted methods and their antifungal activity. Res Chem Inter 40:3085–3093

Shi H, Nagai J, Sakatsume T, Bandow K, Okudaira N, Sakagami H, Tomomura M, Tomomura A, Uesawa Y, Takao K, Sugita Y (2018a) Quantitative structure–cytotoxicity relationship of 2-(N-cyclicamino)chromone derivatives Anticancer Res 38(7):3897–3906. https://doi.org/10.21873/anticanres.12674PMID: 29970510

Shi H, Nagai J, Sakatsume T, Bandow K, Okudaira N, Uesawa Y, Sakagami H, Tomomura M, Tomomura A, Takao K, Sugita Y (2018b) Quantitative structure–cytotoxicity relationship of 3-(N-cyclicamino)chromone derivatives Anticancer Res 38(8):4459–4467

Shimada C, Uesawa Y, Ishii-Nozawa R, Ishihara M, Kagaya H, Kanamto T, Terakubo S, Nakashima H, Takao K, Sugita Y, Sakagami H (2014) Quantitative structure–cytotoxicity relationship of 3-styrylchromones. Anticancer Res 34:5405–5412

Singh P, Anand A, Kumar V (2014) Recent developments in biological activities of chalcones: a mini review. Eur J Med Chem 85:758–777

Thun MJ, DeLancey JO, Center MM, Jemal A, Ward EM (2010) The global burden of cancer: priorities for prevention. Carcinogenesis 31:100–110

Tugrak M, Yamali C, Sakagami H, Gul HI (2016) Synthesis of mono Mannich bases of 2-(4-hydroxybenzylidene)-2,3-dihydroinden-1-one and evaluation of their cytotoxicities. J Enzym Inhib Med Chem 31:818–823

Uesawa Y, Sakagami H, Ishihara M, Kagaya H, Kanamoto T, Terakubo S, Nakashima H, Yahagi H, Takao K, Sugita Y (2015) Quantitative structure–cytotoxicity relationship of 3-styryl-2H-chromenes. Anticancer Res 35:5299–5308

Uesawa Y, Sakagami H, Kagaya H, Yamashita M, Takao K, Sugita Y (2016) Quantitative structure-cytotoxicity relationship of 3-benzylidenechromanones. Anticancer Res 36:5803–5812

Uesawa Y, Sakagami H, Shi H, Hirose M, Takao K, Sugita Y (2018) Quantitative structure-cytotoxicity relationship of furo[2,3-b] chromones. Anticancer Res 38:3283–3290. https://doi.org/10.21873/anticanres.12593. PMID:29848675

Unluer E, Gul HI, Demirtas A, Sakagami H, Umemura N, Tanc M, Kazaz C, Supuran CT (2016) Synthesis and bioactivity studies of 1-aryl-3-(2-hydroxyethylthio)-1-propanones. J Enzym Inhib Med Chem 31:105–109

Varga B, Csonka A, Molnar J, Amaral L, Spengler G (2017) Possible biological and clinical applications of phenothiazines. Anticancer Res 37:5983–5993

Yamali C, Gul HI, Ozgun DO, Sakagami H, Umemura N, Kazaz C, Gul M (2017a) Synthesis and cytotoxic activities of difluoro-dimethoxy chalcones. Anticancer Agents Med Chem 17:1426–1433

Yamali C, Gul HI, Sakagami H, Supuran CT (2016) Synthesis and bioactivities of halogen bearing phenolic chalcones and their corresponding bis Mannich bases. J Enzym Inhib Med Chem 31:125–131

Yamali C, Ozgun DO, Gul HI, Sakagami H, Kazaz C, Okudaira N (2017b) Synthesis and structure elucidation of 1-(2,5/3,5-difluorophenyl)-3-(2,3/2,4/2,5/3,4-dimethoxyphenyl)-2-propen-1-ones as anticancer agents Med Chem Res 26:2017–2023

Yde CW, Clausen MP, Bennetzen MV, Lykkesfeldt AE, Mouritsen OG, Guerra B (2009) The antipsychotic drug chlorpromazine enhances the cytotoxic effect of tamoxifen in tamoxifen-sensitive and tamoxifen-resistant human breast cancer cells. Anticancer Drugs 20:723–735

Yerdelen KO, Gul HI, Sakagami H, Umemura N (2015) Synthesis and biological evaluation of 1,5-bis(4-hydroxy-3-methoxyphenyl) penta-1,4-dien-3-one and its aminomethyl derivatives. J Enzym Inhib Med Chem 30:383–388